

LatentEditor: Text Driven Local Editing of 3D Scenes

Umar Khalid^{1,*}, Hasan Iqbal^{2,*}, Nazmul Karim¹, Jing Hua², Chen Chen¹

¹Center for Research in Computer Vision, University of Central Florida ²Department of Computer Science, Wayne State University
umar.khalid@ucf.edu, hasan.iqbal.cs@wayne.edu, mdnazmul.karim@ucf.edu
jinghua@wayne.edu, chen.chen@crcv.ucf.edu

<https://latenteditor.github.io/>

Abstract

While neural fields have made significant strides in view synthesis and scene reconstruction, editing them poses a formidable challenge due to their implicit encoding of geometry and texture information from multi-view inputs. In this paper, we introduce LATENTEDITOR, an innovative framework designed to empower users with the ability to perform precise and locally controlled editing of neural fields using text prompts. Leveraging denoising diffusion models, we successfully embed real-world scenes into the latent space, resulting in a faster and more adaptable NeRF backbone for editing compared to traditional methods. To enhance editing precision, we introduce a delta score to calculate the 2D mask in the latent space that serves as a guide for local modifications while preserving irrelevant regions. Our novel pixel-level scoring approach harnesses the power of InstructPix2Pix (IP2P) to discern the disparity between IP2P conditional and unconditional noise predictions in the latent space. The edited latents conditioned on the 2D masks are then iteratively updated in the training set to achieve 3D local editing. Our approach achieves faster editing speeds and superior output quality compared to existing 3D editing models, bridging the gap between textual instructions and high-quality 3D scene editing in latent space. We show the superiority of our approach on four benchmark 3D datasets, LLFF [28], IN2N [9], NeRFStudio [43] and NeRF-Art [48].

1. Introduction

The advent of neural radiance fields (NeRF) [29], neural implicit functions [49], and subsequent innovations [20, 31, 47] has revolutionized 3D scene reconstruction and novel view synthesis. These neural fields, leveraging multi-view images and volume/surface rendering mechanisms, have enabled neural networks to implicitly represent both geome-

try and texture of scenes, offering a more reliable and user-friendly alternative to the intricate matching and complex post-processing in traditional methods [19, 52].

While neural fields streamline the digital representation of real-world scenes, editing these fields poses significant challenges. Unlike conventional pixel-space edits [1, 2, 11, 32, 37], editing a NeRF-represented scene requires synchronized editing of multi-views under different perspectives to maintain their consistency, a complex and error-prone task due to the high-dimensional neural network features encoding of shape and texture information. Prior approaches have explored various editing aspects [3, 50, 51], yet they require extensive user interaction. More recent developments, like InstructNeRF2NeRF (IN2N) [9], employ text and image-conditioned models for 3D object creation and editing. However, IN2N struggles with localizing edits.

To tackle this issue, we propose **LatentEditor** that seeks to enhance local editing by predicting the editing area from the editing prompt inside the stable diffusion [38] denoising process, inspired by [24]. Our approach hinges on the critical insight that maintaining consistency in the diffusion feature space is viable and essential for achieving coherent edits in the 3D scene. To this end, we introduce a novel approach to assign delta scores to latent pixels in our designed delta module by contrasting noise predictions from provided instructions against unconditional noise prediction to constrain the local editing. However, projecting these delta scores back to the RGB pixel space introduces inconsistencies. As there is a lack of direct alignment between latent and image pixels, a slight inconsistency in the latent space can affect the NeRF training significantly. Therefore, within our LatentEditor framework, we propose to train NeRF directly within the latent space to enable local latent editing. Our approach, informed by the principles of shape-guided 3D generation in latent space [26], incorporates a refining module that consists of a residual adapter with self-attention to ensure consistency between rendered latent features and the scene’s original latent. During inference, LatentEditor

*Equal Contribution



Figure 1. Our proposed method *LatentEditor* enables text-based NeRF editing (e.g. color, attributes, style, etc.) by instilling both spatial and 3D awareness into image diffusion models. It can be observed in all the results that the background is intact with the color change or style transfer textual prompts. The videos of the rendered scenes are provided in the [supplementary material](#).

Methods	Guidance			Editing Capacity			
	Pre-Computed Masks	Bounding Box	GAN Guidance	Text Driven	Style Transfer	Multi-Attribute Editing	Local Editing
Blend-NeRF [15]	✓	✗	✗	✗	✗	✗	✓
Blended-NeRF [7]	✗	✓	✗	✓	✗	✗	✓
DreamEditor [54]	✓	✗	✗	✓	✓	✗	✓
Control-4D [41]	✗	✗	✓	✓	✗	✗	✗
NeRF-Art [48]	✗	✗	✗	✓	✓	✗	✗
Instruct-N2N [9]	✗	✗	✗	✓	✓	✗	✗
LatentEditor (Ours)	✗	✗	✗	✓	✓	✓	✓

Table 1. **Comparative analysis of prior methods.** Our approach (*LatentEditor*) stands out by not requiring any guidance and showcasing a broader capability for editing, particularly in achieving local edits without reliance on pre-trained segmentation models.

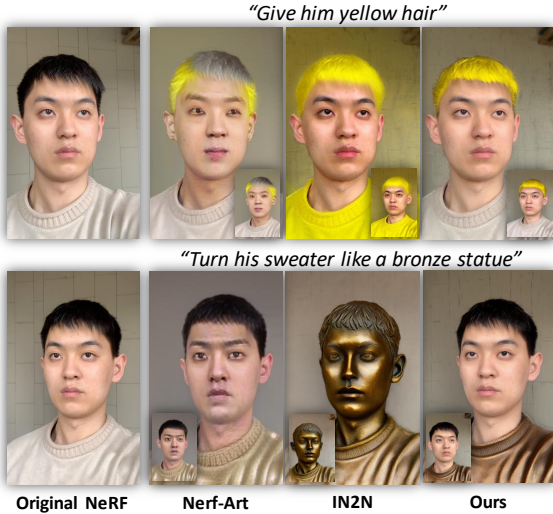


Figure 2. **Local Editing Challenge:** Comparative analysis of local editing capabilities between our *LatentEditor* method and other text-driven 3D NeRF editing approaches, specifically IN2N [9] and NeRF-Art [48]. Our approach preserves the background seamlessly under both editing prompts.

generates a latent representation for specific poses, convertible into RGB images through a Stable Diffusion [38] decoder. The efficacy of *LatentEditor* is evident in Figure 1, showcasing its capability for precise and minimal local edits in 3D NeRF scenes. The primary **contributions** of this paper are as follows:

- We introduce an efficient text-driven 3D NeRF local editing framework that operates solely based on text prompts, eliminating the need for additional controls. This innovation marks a significant advancement in text-driven 3D scene editing.
- Our unique delta module, utilizing the InstructPix-toPix [2] backbone, enables a novel mechanism for local editing. Guided solely by editing prompts, it efficiently calculates 2D masks in the latent space, automatically constraining targeted modifications in precise locations.
- In our efficient NeRF editing method, NeRF operates directly in its latent space, reducing computational costs significantly. In addition, our designed delta module further limits the required number of editing iterations, resulting in up to a 5-fold reduction in editing time compared to the baseline IN2N [9].
- A newly introduced refining module, featuring a trainable adapter with residual and self-attention mechanism, ensures enhanced consistency in the integration of latent masks within latent NeRF training. This adapter is key in aligning rendered latent features with the scene’s original latents, resolving unwanted inconsistencies.

Extensive experiments on four 3D datasets and practical applications demonstrate our framework’s capability to achieve spatially and semantically consistent performance and precise multi-attribute local editing in 3D scenes, vali-

dating the effectiveness of *LatentEditor*.

2. Related Work

Recent advancements in denoising diffusion probabilistic models [11, 42] have enabled the generation of high-quality images based on complex text cues [37–39]. These models have been further refined for text-driven image editing, with significant contributions made by [1, 5, 10, 13]. Notably, SDEdit [25] and DiffEdit [5] have laid the groundwork for using denoising diffusion in image editing, despite certain limitations in preserving original image details or handling complex captions. These developments have paved the way for novel 3D scene synthesis, particularly with the incorporation of text-to-image models like CLIP [35] in DreamField [12] and DreamFusion [34]. Initiating with DreamFusion [34], a series of subsequent methods [21, 26, 36] demonstrated noteworthy outcomes using diffusion-based priors. However, these methods are circumscribed to generating ‘novel’ 3D scenes, making them inapplicable to our focus on NeRF-editing, which aims to modify existing 3D scenes based on provided conditions.

Compared to the task of novel object generation, the editing of NeRF remains a less-explored area owing to its inherent complexity. Initial efforts in this domain focused on color, geometric, and style modifications [8, 17, 22, 46, 53]. The integration of text-to-image diffusion models has been a recent trend in NeRF editing, with methodologies like Score Distillation Sampling in DreamFusion [34], and regularization approaches in Vox-e [40] and NeRF-Art [48].

Notably, InstructNeRF2NeRF (IN2N) [9] utilized 2D image translation models for NeRF editing based on text prompts but faced issues with over-editing. To address this, DreamEditor [54] introduced a mesh-based approach for more focused edits, using pre-computed masks. Similarly, Blended-NeRF [7] and Blend-NeRF [15] incorporated additional cues like bounding boxes for localized adjustments.

In our approach, we innovate by integrating latent space NeRF training with a unique delta module leveraging diffusion models to generate editing masks. Our approach enables precise local editing without extra guidance. The architecture of the delta module is heavily influenced by another recent work [30]. Also, another recent work [33] highlights the significance of latent NeRF editing. The comparative analysis (Table 1 and Figure 2) showcases our framework’s superior local editing compared to existing text-driven NeRF methods.

3. Method

Our objective is to introduce a text-prompt-driven approach that enables efficient and effective local editing of real-world 3D scenes. Our method, as illustrated in Figure 3, commences by optimizing a Neural Radiance Field (NeRF)

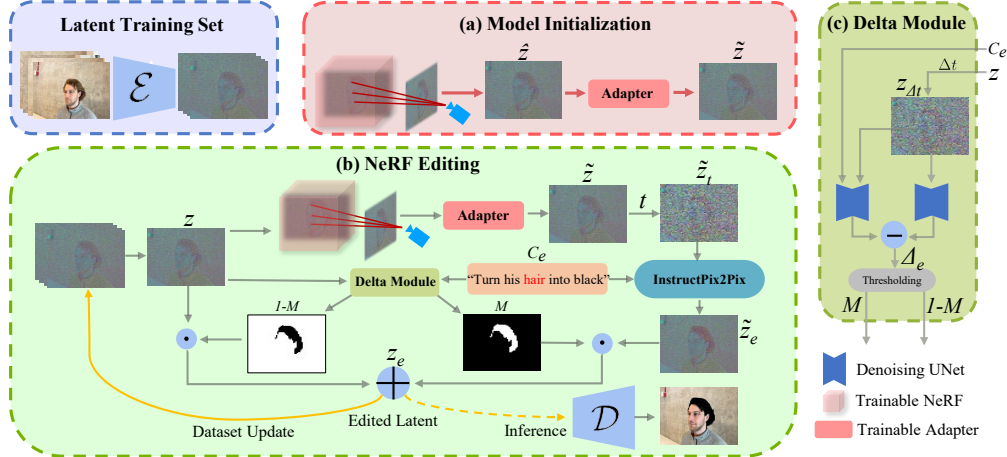


Figure 3. **Overall pipeline of LatentEditor for model initialization and editing.** (a) We initialize the NeRF model within the latent domain, guided by the latent features of the original dataset. Our refinement adapter mitigates the misalignment in the latent space and encompasses a trainable adapter with residual and self-attention mechanisms. (b) Upon initialization, LatentEditor iteratively refines the model within the latent space for a predetermined number of iterations, while consistently updating the training set with the edited latents, Z_e . (c) The Delta Module is adept at interpreting prompts and produces the mask for targeted editing. Additionally, it integrates the denoising U-Net from IP2P [2]. However, Δt used in calculating delta scores Δ_e is a hyperparameter and is different from t which is randomly selected. An RGB image can be obtained by feeding the edited latent to the stable diffusion (SD) [38] decoder \mathcal{D} whereas \mathcal{E} represents SD [38] encoder.

within the latent space delineated by Stable Diffusion [38], thus anchoring the scene representation using latent feature vectors (see Figure 3(a)). We further introduce a refinement adapter module designed to augment NeRF’s capability in synthesizing novel views, yielding more coherent and high-fidelity results.

For scene editing, we present an innovative approach to facilitate localized editing using unconditional edits within the framework of the IP2P [2] model (see Figure 3(b)). Such unconditional edits helps compute latent masks within our distinctive delta module as illustrated in Figure 3(c). Original latents are edited through the guidance of the masks and prompt, and iterative Dataset-Update DU [9] is performed in the latent space. Once NeRF is trained with latent features, latent representations can then be processed through a Stable Diffusion decoder [38] to realize the scene editing.

3.1. Background

InstructPix2Pix IP2P [2] edits an input image I based on a textual editing instruction C_e . Leveraging latent diffusion techniques [38] and a Variational Autoencoder (VAE) with an encoder \mathcal{E} and decoder \mathcal{D} , IP2P processes a noisy image latent z_t . It predicts a less noisy version z_0 by approximating the noise vector $\hat{\epsilon}$ using a U-Net ε_θ :

$$\hat{\epsilon} = \varepsilon_\theta(z_t, I, C_e), \quad (1)$$

where $t \in T$ represents the noise level. IP2P is trained under various conditions, enabling both conditional and unconditional denoising.

Neural Radiance Fields NeRF [29] uses Multi-Layer Perceptrons (MLPs) to estimate the density σ and color \mathbf{c}

for a given 3D voxel $\mathbf{p} = (p_x, p_y, p_z)$ and view direction \mathbf{v} . After transforming \mathbf{p} and \mathbf{v} into high-frequency vectors via positional encoding $\phi(\cdot)$, NeRF produces

$$(\mathbf{c}, \sigma) = F_\theta^c(\phi(\mathbf{p}), \phi(\mathbf{v})). \quad (2)$$

NeRF calculates the world-space ray $\mathbf{r}(\tau) = \mathbf{c} + \tau\mathbf{v}$ per image pixel and minimizes the difference between rendered and captured pixel colors through the loss $\mathcal{L}(C(\mathbf{r}), \hat{C}(\mathbf{r}))$.

InstructNeRF2NeRF IN2N [9] fine-tunes reconstructed NeRF models using editing instructions to create modified scenes. It employs an iterative Dataset-Update (DU) strategy, where dataset images are successively replaced with post-editing. This process enables the diffusion priors’ gradual integration into the 3D scene. IN2N [9] uses an image-conditioned diffusion model, IP2P [2], and is a modified implementation of score distillation sampling (SDS) [34]. The DU strategy in IN2N [9] is superior to the naive SDS implementation for NeRF editing, forming the basis for our approach of substituting training samples with edited latents.

3.2. LatentEditor for NeRF Editing

LatentEditor correlates semantics from editing text prompts with local geometry in latent space and then optimizes a Neural Radiance Field (NeRF) for localized editing. Our method consists of two stages: Model Initialization and NeRF Editing.

3.2.1 Model Initialization

Given a dataset of multi-view images $\mathbf{I} \in \mathbb{R}^{N \times W \times H \times 3}$, we encode these images using an encoder, \mathcal{E} , to obtain latent features $z^n = \mathcal{E}(I^n) \in \mathbb{R}^{W' \times H' \times 4}$ for $W' < W$ and $H' < H$. These latent feature maps $\mathbf{Z} := \{z^n\}_{n=1}^N$ serve as labels for initial LatentEditor NeRF training. We redefine the volume rendering integral as follows:

$$\hat{Z}(\mathbf{r}) = \int_{\tau_n}^{\tau_f} \mathbf{T}(\tau) \sigma(\mathbf{r}(\tau)) \mathbf{z}(\mathbf{r}(\tau), \mathbf{d}) d\tau, \quad (3)$$

where $\mathbf{T}(\tau)$ is the accumulated transmittance, $\sigma(\mathbf{r}(\tau))$ is the density, and $\mathbf{z}(\mathbf{r}(\tau), \mathbf{d})$ is the radiance emitted at $\mathbf{r}(\tau)$.

The reconstruction loss, as the difference between estimated and actual pixel latent values, is defined by:

$$\mathcal{L}_r = \sum_{\mathbf{r} \in \mathcal{R}} \|\hat{Z}(\mathbf{r}) - Z(\mathbf{r})\|^2, \quad (4)$$

The NeRF model F_θ^z is trained to predict both latent features \mathbf{z} and density σ from encoded positions and directions:

$$(\mathbf{z}, \sigma) = F_\theta^z(\phi(\mathbf{p}), \phi(\mathbf{v})). \quad (5)$$

Refinement Adapter with Self-Attention. Our refinement module, addressing misalignment in latent space, includes a trainable adapter for real-world 3D scene editing. It performs the following residual and self-attention operations on an input tensor $\hat{z} \in \mathbb{R}^{4 \times h' \times w'}$:

$$z_{\text{attention}} = \text{SelfAttention}(\text{ConvDown}(\hat{z})) \quad (6)$$

$$\tilde{z} = \hat{z} + \text{ConvUp}(z_{\text{attention}}) \quad (7)$$

The refinement loss for pixel latent vector \tilde{Z}^i from refined feature map \tilde{z}^i is:

$$\mathcal{L}_f = \sum_{\mathbf{r} \in \mathcal{R}} \left\| \tilde{Z}^i(\mathbf{r}) - Z^i(\mathbf{r}) \right\|^2, \quad (8)$$

where $\tilde{z}^i = F_\Theta(\hat{z}^i)$.

The total training loss combines refinement and reconstruction losses:

$$\mathcal{L}_T = \lambda_r \mathcal{L}_r + \lambda_f \mathcal{L}_f. \quad (9)$$

We concurrently update NeRF (F_θ) and the refinement adapter (F_Θ) by minimizing \mathcal{L}_T for various view reconstructions.

3.2.2 NeRF Editing

After initializing the NeRF model in the latent domain with features $\mathbf{Z} = \{z^n\}_{n=1}^N$, we employ the InstructPix2Pix (IP2P) framework [2] to align its parameters with the textual cue C_e . The original latent variables \mathbf{Z} are systematically replaced with edited versions $\mathbf{Z}_e = \{z_e^n\}_{n=1}^N$ at an

editing rate ν , enabling progressive transformation to reflect desired edits. For viewpoint K and editing iteration s , we obtain a render, \tilde{z}^n from F_θ^z and generate edited latents z_e^n using our novel local editing technique.

Prompt Aware Pixel Scoring. We design a delta module by modulating the IP2P [2] diffusion process that aims to guide the generation of z_e^n using a generated mask. Starting with noise addition to latent z^n up to timestep Δt , we obtain the noisy latent $z_{\Delta t}^n$ as:

$$z_{\Delta t}^n = \sqrt{\beta_{\Delta t}} z^n + \sqrt{1 - \beta_{\Delta t}} \varepsilon, \quad (10)$$

where $\varepsilon \sim \mathcal{N}(0, 1)$, and β_t is the noise scheduling factor at timestep t .

IP2P's score estimation encompasses conditional and unconditional editing:

$$\begin{aligned} \tilde{\varepsilon}_\theta(z_t, I, C_e) &= \varepsilon_\theta(z_t, \emptyset_I, \emptyset_e) \\ &+ s_I(\varepsilon_\theta(z_t, I, \emptyset_e) - \varepsilon_\theta(z_t, \emptyset_I, \emptyset_e)) \\ &+ s_T(\varepsilon_\theta(z_t, I, C_e) - \varepsilon_\theta(z_t, I, \emptyset_e)). \end{aligned} \quad (11)$$

We calculate the delta scores, Δ_ε , using two noise predictions:

$$\Delta_\varepsilon = |\varepsilon_\theta(z_{\Delta t}^n, I, C_e) - \varepsilon_\theta(z_{\Delta t}^n, I, \emptyset_e)| \quad (12)$$

where $z_{\Delta t}^n$ is calculated using Equation 10, and Δt is a hyperparameter in our method.

The higher values of the delta scores, $\Delta_\varepsilon \in \mathbb{R}^{W' \times H' \times 4}$ indicate the region to be edited. Hence, a binary mask, $M \in \mathbb{R}^{W' \times H' \times 4}$ can be generated by applying a threshold μ on Δ_ε as following,

$$M = \begin{cases} 1 & \text{if } \Delta_\varepsilon \geq \mu \\ 0 & \text{otherwise} \end{cases}$$

Since M is generated in the latent space, we will perform the local editing by refining the NeRF on edited latents as discussed in the following section.

Local Editing with Latent Features Once the delta module outputs the mask M , a noisy version \tilde{z}_t^n of the current render is generated, where t now has a random value in a specific range $[t_{min}, t_{max}]$. The edited latent $\tilde{z}_{t-1,e}^n$ at timestep $t-1$, is computed using DDIM [42]:

$$\tilde{z}_{t-1,e}^n = \sqrt{\beta_{t-1}} \left(\frac{\tilde{z}_t^n - \sqrt{1 - \beta_t} \tilde{\varepsilon}_t}{\sqrt{\beta_t}} \right) + \sqrt{1 - \beta_{t-1}} \tilde{\varepsilon}_t. \quad (13)$$

where $\tilde{\varepsilon}_t = \tilde{\varepsilon}_\theta(\tilde{z}_t, I, C_e)$ is the predicted noise. Iteratively applying these denoising stages yields the edited latent z_e^n .

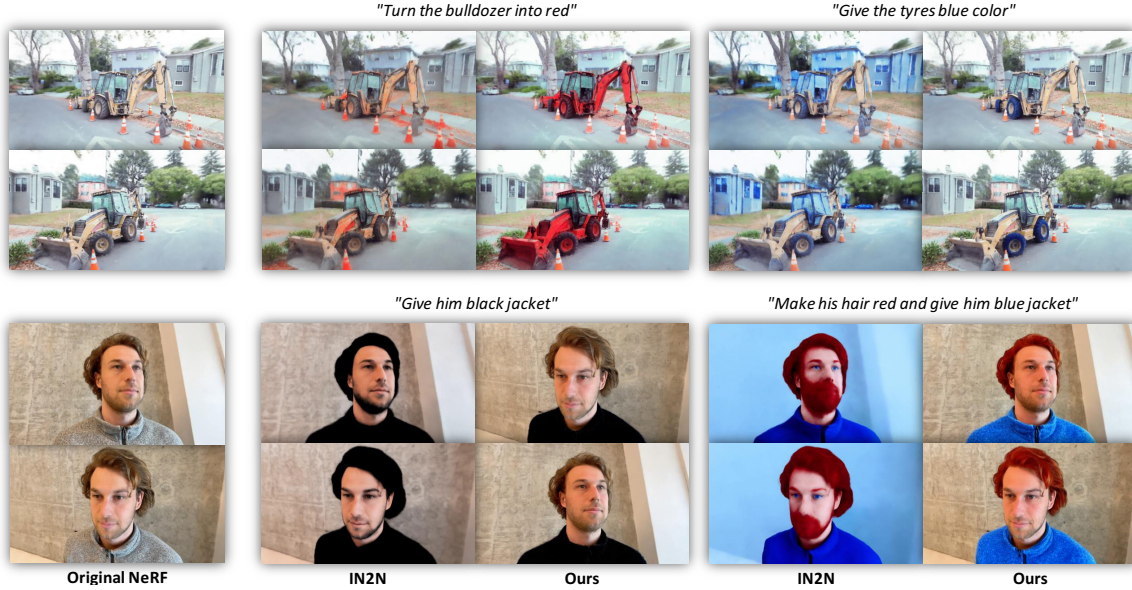


Figure 4. **Qualitative Results.** The visual results of our approach, when contrasted with the baseline IN2N [9] across two distinct scenes, distinctly demonstrate that *LatentEditor* excels in accurately pinpointing the pertinent region, executing faithful text edits, and averting undesired alterations. These achievements prove challenging for the baseline method [9] to replicate effectively as IN2N [9] also changes the background objects’ color to blue given that the editing prompt, “Give the tyres blue color” only wants the tyre color to be changed.



Figure 5. **Style Transfer Comparison.** We present a visual representation for stylization editing, comparing our results with those obtained using NeRF-Art [48] and Instruct-NeRF2NeRF [9]. Our results look similar to IN2N [9] as it also uses IP2P [2] editing framework. However, it can be observed that *LatentEditor* keeps the background intact while transferring the style of an object.

The final prediction \tilde{z}_e^n after complete denoising merges with z^n using the mask M :

$$z_e^n = \tilde{z}_e^n \odot M + (1 - M) \odot z^n \quad (14)$$

Ultimately, for each n in the set $\{1, \dots, N\}$, the locally edited latent z_e^n is substituted for the original z^n in an iterative fashion.

This method ensures that pixels outside the edit mask M remain unaltered, confining edits to the intended regions.

Optimizing NeRF Editing. We don’t incorporate any additional preservation or density blending losses within our methodology. The loss defined in Equation 9 suffices for NeRF editing with DU, where the ground truth is continuously updated with edited latents. Our approach avoids the extensive hyperparameter tuning required by other NeRF editing methods [7, 15, 27].

Multi-attribute Editing. We also expand our method to tackle a more challenging multi-attribute editing task in NeRF. Our approach can be seamlessly integrated with any pre-trained grounding framework, such as GLIP [18]. However, given that the grounding mechanism is inherently embedded within our delta module, we performed prompt engineering for LLM [45].

For instance, employing our designed prompt, LLM [45] processes the input “Make his hair red and give him a blue jacket,” yielding the output {[“Make his hair red”, “Give him a blue jacket”], 2}. Our delta module is designed to be aware of LLM output, generating M^1 and M^2 based on C_e^1 and C_e^2 , respectively which further controls multi-edit in a single scene. To achieve multi-attribute editing, we leverage pre-trained large language model (LLM) Llama 2 [45]. To achieve our multi-attribute editing, we feed in the given prompt C_e to the LLM, and the LLM output is engineered in a way that our proposed delta-module can generate multiple masks.

Here is the designed prompt used in the study:

```

1 ### Contexts
2 Break the following editing prompt into multiple
  parts with "and" as the key indicator of
  partition. Produce editing prompts based on
  the given input.
3 ### Input
4 Make his hair red and give him blue jacket.
5 ### Response

```

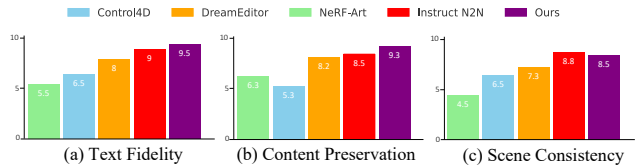


Figure 6. **User Study.** In a comprehensive user study encompassing three evaluation criteria, LatentEditor achieves the highest text fidelity and content preservation scores while IN2N [9] score higher on 3D consistency criteria.

4. Experimental Analysis

Implementation Details In our experiments, we adopt the implementation strategy of IN2N [9], specifically setting the interval $[t_{\min}, t_{\max}] = [0.02, 0.98]$ and defining $\Delta t = 0.75$. Model initialization on the original scene is performed for 30,000 iterations, ensuring a robust baseline representation. The editing process then commences, with the number of iterations tailored to the number of training views ranging from 2,000 iterations to 4,000. Detailed descriptions of these settings are available in the [supplementary material](#).

Method	CLIP Text-Image Direction Similarity \uparrow	CLIP Direction Consistency \uparrow	Edit PSNR \uparrow
NeRF-Art [48]	0.2755	0.9672	22.15
Control4D [41]	0.2503	0.9751	20.89
DreamEditor [54]	0.2604	0.9802	21.76
IN2N [9]	0.2788	0.9850	25.34
Ours	0.2801	0.9881	26.47

Table 2. Quantitative evaluation of scene edits in terms of text alignment and frame consistency in CLIP space where our approach demonstrates the highest consistency.

Baselines For a comprehensive evaluation of LatentEditor’s performance, we compared it against state-of-the-art (SOTA) models across four datasets: (i) IN2N [9], (ii) NeRF-Art [48], (iii) LLFF [28] and (iv) NeRFstudio Dataset [43]. We included various NeRF editing frameworks in our analysis, such as IN2N [9], NeRF-Art [48], Control-4D [41], and DreamEditor [54]. However, due to space constraints, we primarily emphasize qualitative comparisons with IN2N [9], the current benchmark in text-driven NeRF editing.

4.1. Results

Quantitative Quantitative evaluations, as detailed in Table 2, involved 56 edits across 14 scenes from the above-mentioned four datasets. Our method outperformed baselines in CLIP similarity scores and CLIP direction consistency, as averaged over multiple views rendered from NeRF. This superiority in scoring demonstrates the precision of LatentEditor in aligning edited NeRF scenes with target text conditions.

User Study To evaluate the subjective nature of scene editing, we conducted a user study comparing our method with SOTA alternatives. The study garnered a total of 500 votes across three key metrics: 3D consistency, preservation of original scene content, and adherence to text descriptions. As depicted in Figure 6, our method has been predominantly favored across these metrics.

Further details on the quantitative evaluation criteria and implementation of this user study are available in the [supplementary material](#).

Qualitative Our method’s unified editing capability is distinctly showcased in Figure 1. Furthermore, Figure 2 demonstrates LatentEditor’s enhanced local editing prowess when juxtaposed with SOTA IN2N [9] approach. A notable distinction is observed in Figure 4, where our method adeptly adheres to the prompt “Give him Black Jacket”, unlike IN2N [9] which erroneously alters the hair color. Although style transfer results from both LatentEditor and IN2N [9] are comparable, as seen in Figure 5, due to their shared IP2P [2] backbone, LatentEditor exhibits more refined control. The versatility of LatentEditor in managing

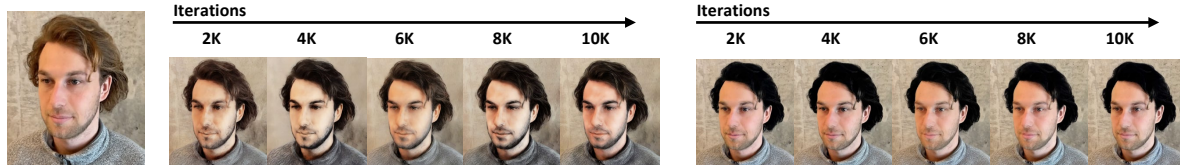


Figure 7. Comparing *LatentEditor* to IN2N in terms of a reduced computational cost, our goal is to minimize the number of training iterations required with a higher editing rate (fewer IP2P calls). Our approach achieves the desired editing results, “Turn his hair black”, in approximately 2000 iterations, whereas IN2N continues to face challenges even after 10,000 iterations.



Figure 8. Qualitative comparison of an edited image with and without refinement loss against the editing prompt, “turn his hair black”. The red box indicates the noticeable artifacts without the refinement module.

complex prompts and multi-attribute edits is further highlighted in Figure 4, underscoring its robustness in diverse editing scenarios.

5. Ablations

Editing Rate vs Training Iterations In this ablation study, we evaluate the computational efficiency of our *LatentEditor* approach against IN2N [9], particularly in terms of training iterations required to achieve a targeted editing performance. As illustrated in Figure 7, using the editing prompt “Turn his hair black”, we demonstrate that *LatentEditor* significantly outperforms IN2N [9] in computational cost. Specifically, our method achieves the desired editing results with an approximately five to ten-fold reduction in training iterations. *LatentEditor* requires only about 2000 iterations to reach the editing rate benchmark, while IN2N [9] still faces challenges even after 10,000 iterations. Despite *LatentEditor* involves multiple denoising stages per editing step, which increases the cost per step, it achieves the de-



Figure 9. Our method grapples with instructions like “Turn the bear into an orange bear” due to IP2P’s limitations, while *LatentEditor*’s model-agnostic approach offers promise for addressing such issues through enhanced instruction-conditioned diffusion models.

sired performance with significantly fewer iterations. As a result, it is **5-8** times faster in NeRF editing compared to IN2N [9]. A more detailed analysis of this experiment is provided in the [supplementary material](#).

Refinement Coefficient Sensitivity To understand the impact of the refinement module, we conduct an ablation study on the refinement coefficient where this coefficient is set to zero. The results, as illustrated in Figure 8, reveal that omitting the refinement leads to noticeable inconsistencies and artifacts in the NeRF scene. These findings highlight the importance of the refinement loss in achieving high-quality, consistent NeRF scenes and validate its inclusion in our loss formulation.

6. Limitations

Our method’s efficacy is contingent on the capabilities of the pre-trained IP2P model [2], which presents certain limitations. This is particularly evident in cases where IP2P’s inherent weaknesses are pronounced. For instance, in Figure 9, the prompt “Turn the bear into an orange bear” exemplifies such a scenario. While IN2N [9] introduces random coloring throughout the scene, failing to generate the desired NeRF, our method, though demonstrating more controlled editing, does not completely succeed in turning the bear orange. The underlying limitation stems from IP2P’s challenges in accurately interpreting and executing specific editing instructions like this.

Our approach, being model-agnostic, can benefit from future enhancements in instruction-conditioned diffusion models, potentially overcoming these current constraints in localized edits.

7. Conclusion

In conclusion, *LatentEditor* marks a significant advancement in the field of neural field editing. We tackled the inherent challenges in editing neural fields, which arise from their implicit encoding of geometry and texture, by introducing a novel framework capable of precise, controlled editing via text prompts. By embedding real-world scenes into latent space using denoising diffusion models, our framework offers a faster and more adaptable NeRF

backbone for text-driven editing. The introduction of the delta score, which calculates 2D masks in latent space for precise editing while preserving untargeted areas, is a key innovation. LatentEditor not only simplifies the process of 3D scene editing with textual instructions but also enhances the quality of the results, marking a new direction in 3D content creation and modification.

References

- [1] Omri Avrahami, Dani Lischinski, and Ohad Fried. Blended diffusion for text-driven editing of natural images. In *CVPR 2022*, pages 18208–18218, 2022. [1](#), [3](#)
- [2] Tim Brooks, Aleksander Holynski, and Alexei A Efros. Instructpix2pix: Learning to follow image editing instructions. *arXiv preprint arXiv:2211.09800*, 2022. [1](#), [3](#), [4](#), [5](#), [6](#), [7](#), [8](#), [11](#), [15](#)
- [3] Jianchuan Chen, Ying Zhang, Di Kang, Xuefei Zhe, Linchao Bao, Xu Jia, and Huchuan Lu. Animatable neural radiance fields from monocular rgb videos. *arXiv preprint arXiv:2106.13629*, 2021. [1](#)
- [4] Zhe Chen, Yuchen Duan, Wenhai Wang, Junjun He, Tong Lu, Jifeng Dai, and Yu Qiao. Vision transformer adapter for dense predictions. *arXiv preprint arXiv:2205.08534*, 2022. [12](#)
- [5] Guillaume Couairon, Jakob Verbeek, Holger Schwenk, and Matthieu Cord. Diffedit: Diffusion-based semantic image editing with mask guidance. *arXiv preprint arXiv:2210.11427*, 2022. [3](#)
- [6] Rinon Gal, Or Patashnik, Haggai Maron, Gal Chechik, and Daniel Cohen-Or. Stylegan-nada: Clip-guided domain adaptation of image generators. *arXiv preprint arXiv:2108.00946*, 2021. [15](#)
- [7] Ori Gordon, Omri Avrahami, and Dani Lischinski. Blended-nerf: Zero-shot object generation and blending in existing neural radiance fields. *arXiv preprint arXiv:2306.12760*, 2023. [2](#), [3](#), [6](#)
- [8] Jiatao Gu, Lingjie Liu, Peng Wang, and Christian Theobalt. Stylenerf: A style-based 3d-aware generator for high-resolution image synthesis. *arXiv preprint arXiv:2110.08985*, 2021. [3](#)
- [9] Ayaan Haque, Matthew Tancik, Alexei A Efros, Aleksander Holynski, and Angjoo Kanazawa. Instruct-nerf2nerf: Editing 3d scenes with instructions. *arXiv preprint arXiv:2303.12789*, 2023. [1](#), [2](#), [3](#), [4](#), [6](#), [7](#), [8](#), [11](#), [12](#), [13](#), [14](#), [15](#)
- [10] Amir Hertz, Ron Mokady, Jay Tenenbaum, Kfir Aberman, Yael Pritch, and Daniel Cohen-Or. Prompt-to-prompt image editing with cross attention control. *arXiv preprint arXiv:2208.01626*, 2022. [3](#)
- [11] Jonathan Ho, Ajay Jain, and Pieter Abbeel. Denoising diffusion probabilistic models. *Advances in Neural Information Processing Systems*, 33:6840–6851, 2020. [1](#), [3](#)
- [12] Ajay Jain, Ben Mildenhall, Jonathan T Barron, Pieter Abbeel, and Ben Poole. Zero-shot text-guided object generation with dream fields. In *Proceedings of the IEEE/CVF Conference on Computer Vision and Pattern Recognition*, pages 867–876, 2022. [3](#)
- [13] Bahjat Kawar, Shiran Zada, Oran Lang, Omer Tov, Huiwen Chang, Tali Dekel, Inbar Mosseri, and Michal Irani. Imagic: Text-based real image editing with diffusion models. *arXiv preprint arXiv:2210.09276*, 2022. [3](#)
- [14] Umar Khalid, Hasan Iqbal, Saeed Vahidian, Jing Hua, and Chen Chen. Cefhri: A communication efficient federated learning framework for recognizing industrial human-robot interaction. *arXiv preprint arXiv:2308.14965*, 2023. [12](#)
- [15] Hyunsu Kim, Gayoung Lee, Yunjey Choi, Jin-Hwa Kim, and Jun-Yan Zhu. 3d-aware blending with generative nerfs. *arXiv preprint arXiv:2302.06608*, 2023. [2](#), [3](#), [6](#)
- [16] Alexander Kirillov, Eric Mintun, Nikhila Ravi, Hanzi Mao, Chloe Rolland, Laura Gustafson, Tete Xiao, Spencer Whitehead, Alexander C Berg, Wan-Yen Lo, et al. Segment anything. *arXiv preprint arXiv:2304.02643*, 2023. [11](#), [15](#)
- [17] Zhengfei Kuang, Fujun Luan, Sai Bi, Zhixin Shu, Gordon Wetzstein, and Kalyan Sunkavalli. Palettenerf: Palette-based appearance editing of neural radiance fields. In *Proceedings of the IEEE/CVF Conference on Computer Vision and Pattern Recognition*, pages 20691–20700, 2023. [3](#)
- [18] Liunian Harold Li, Pengchuan Zhang, Haotian Zhang, Jianwei Yang, Chunyuan Li, Yiwu Zhong, Lijuan Wang, Lu Yuan, Lei Zhang, Jenq-Neng Hwang, et al. Grounded language-image pre-training. In *Proceedings of the IEEE/CVF Conference on Computer Vision and Pattern Recognition*, pages 10965–10975, 2022. [7](#)
- [19] Hao-Kang Liu, I Shen, Bing-Yu Chen, et al. Nerf-in: Free-form nerf inpainting with rgb-d priors. *arXiv preprint arXiv:2206.04901*, 2022. [1](#)
- [20] Lingjie Liu, Jiatao Gu, Kyaw Zaw Lin, and et al. Neural sparse voxel fields. *NeurIPS 2020*, 33:15651–15663, 2020. [1](#)
- [21] Ruoshi Liu, Rundi Wu, Basile Van Hoorick, Pavel Tokmakov, Sergey Zakharov, and Carl Vondrick. Zero-1-to-3: Zero-shot one image to 3d object, 2023. [3](#)
- [22] Steven Liu, Xiuming Zhang, Zhoutong Zhang, Richard Zhang, Jun-Yan Zhu, and Bryan Russell. Editing conditional radiance fields. In *Proceedings of the IEEE/CVF international conference on computer vision*, pages 5773–5783, 2021. [3](#)
- [23] Timo Lüddecke and Alexander Ecker. Image segmentation using text and image prompts. In *Proceedings of the IEEE/CVF Conference on Computer Vision and Pattern Recognition*, pages 7086–7096, 2022. [11](#)
- [24] Andreas Lugmayr, Martin Danelljan, Andres Romero, Fisher Yu, Radu Timofte, and Luc Van Gool. Repaint: Inpainting using denoising diffusion probabilistic models. In *Proceedings of the IEEE/CVF Conference on Computer Vision and Pattern Recognition*, pages 11461–11471, 2022. [1](#)
- [25] Chenlin Meng, Yutong He, Yang Song, Jiaming Song, Jiajun Wu, Jun-Yan Zhu, and Stefano Ermon. Sdedit: Guided image synthesis and editing with stochastic differential equations. *arXiv preprint arXiv:2108.01073*, 2021. [3](#)
- [26] Gal Metzer, Elad Richardson, Or Patashnik, Raja Giryes, and Daniel Cohen-Or. Latent-nerf for shape-guided generation of 3d shapes and textures. *arXiv preprint arXiv:2211.07600*, 2022. [1](#), [3](#), [11](#), [12](#)

- [27] Aryan Mikaeili, Or Perel, Mehdi Safaee, Daniel Cohen-Or, and Ali Mahdavi-Amiri. Sked: Sketch-guided text-based 3d editing. In *Proceedings of the IEEE/CVF International Conference on Computer Vision*, pages 14607–14619, 2023. [6](#)
- [28] Ben Mildenhall, Pratul P Srinivasan, Rodrigo Ortiz-Cayon, Nima Khademi Kalantari, Ravi Ramamoorthi, Ren Ng, and Abhishek Kar. Local light field fusion: Practical view synthesis with prescriptive sampling guidelines. *ACM Transactions on Graphics (TOG)*, 38(4):1–14, 2019. [1](#), [7](#)
- [29] Ben Mildenhall, Pratul P Srinivasan, Matthew Tancik, Jonathan T Barron, Ravi Ramamoorthi, and Ren Ng. Nerf: Representing scenes as neural radiance fields for view synthesis. *Communications of the ACM*, 65(1):99–106, 2021. [1](#), [4](#)
- [30] Ashkan Mirzaei, Tristan Aumentado-Armstrong, Marcus A Brubaker, Jonathan Kelly, Alex Levinshtein, Konstantinos G Derpanis, and Igor Gilitschenski. Watch your steps: Local image and scene editing by text instructions. *arXiv preprint arXiv:2308.08947*, 2023. [3](#)
- [31] Thomas Müller, Alex Evans, Christoph Schied, and Alexander Keller. Instant neural graphics primitives with a multiresolution hash encoding. *ACM Transactions on Graphics (ToG)*, 41(4):1–15, 2022. [1](#)
- [32] Alex Nichol, Prafulla Dhariwal, Aditya Ramesh, Pranav Shyam, Pamela Mishkin, Bob McGrew, Ilya Sutskever, and Mark Chen. Glide: Towards photorealistic image generation and editing with text-guided diffusion models. *arXiv preprint arXiv:2112.10741*, 2021. [1](#)
- [33] Jangho Park, Gihyun Kwon, and Jong Chul Ye. Ed-nerf: Efficient text-guided editing of 3d scene using latent space nerf. *arXiv preprint arXiv:2310.02712*, 2023. [3](#)
- [34] Ben Poole, Ajay Jain, Jonathan T Barron, and Ben Mildenhall. Dreamfusion: Text-to-3d using 2d diffusion. *arXiv preprint arXiv:2209.14988*, 2022. [3](#), [4](#)
- [35] Alec Radford, Jong Wook Kim, Chris Hallacy, Aditya Ramesh, Gabriel Goh, Sandhini Agarwal, Girish Sastry, Amanda Askell, Pamela Mishkin, Jack Clark, et al. Learning transferable visual models from natural language supervision. In *International conference on machine learning*, pages 8748–8763. PMLR, 2021. [3](#)
- [36] Amit Raj, Srinivas Kaza, Ben Poole, Michael Niemeyer, Nataniel Ruiz, Ben Mildenhall, Shiran Zada, Kfir Aberman, Michael Rubinstein, Jonathan Barron, et al. Dreambooth3d: Subject-driven text-to-3d generation. *arXiv preprint arXiv:2303.13508*, 2023. [3](#)
- [37] Aditya Ramesh, Prafulla Dhariwal, Alex Nichol, Casey Chu, and Mark Chen. Hierarchical text-conditional image generation with clip latents. *arXiv preprint arXiv:2204.06125*, 2022. [1](#), [3](#)
- [38] Robin Rombach, Andreas Blattmann, Dominik Lorenz, Patrick Esser, and Björn Ommer. High-resolution image synthesis with latent diffusion models. In *CVPR 2022*, pages 10684–10695, 2022. [1](#), [3](#), [4](#), [11](#), [12](#)
- [39] Chitwan Saharia, William Chan, and Saurabh et al. Saxena. Photorealistic text-to-image diffusion models with deep language understanding. *NeurIPS 2022*, 35:36479–36494, 2022. [3](#)
- [40] Etai Sella, Gal Fiebelman, Peter Hedman, and Hadar Averbuch-Elor. Vox-e: Text-guided voxel editing of 3d objects. *arXiv preprint arXiv:2303.12048*, 2023. [3](#)
- [41] Ruizhi Shao, Jingxiang Sun, Cheng Peng, Zerong Zheng, Boyao Zhou, Hongwen Zhang, and Yebin Liu. Control4d: Dynamic portrait editing by learning 4d gan from 2d diffusion-based editor. *arXiv preprint arXiv:2305.20082*, 2023. [2](#), [7](#), [14](#)
- [42] Jiaming Song, Chenlin Meng, and Stefano Ermon. Denoising diffusion implicit models. *arXiv preprint arXiv:2010.02502*, 2020. [3](#), [5](#)
- [43] Matthew Tancik, Ethan Weber, Evonne Ng, Ruilong Li, Brent Yi, Terrance Wang, Alexander Kristoffersen, Jake Austin, Kamyar Salahi, Abhik Ahuja, et al. Nerfstudio: A modular framework for neural radiance field development. In *ACM SIGGRAPH 2023 Conference Proceedings*, pages 1–12, 2023. [1](#), [7](#), [12](#)
- [44] Katrin Tomanek, Vicky Zayats, Dirk Padfield, Kara Vaillancourt, and Fadi Biadisy. Residual adapters for parameter-efficient asr adaptation to atypical and accented speech. *arXiv preprint arXiv:2109.06952*, 2021. [12](#)
- [45] Hugo Touvron, Louis Martin, Kevin Stone, Peter Albert, Amjad Almahairi, Yasmine Babaei, Nikolay Bashlykov, Soumya Batra, Prajjwal Bhargava, Shruti Bhosale, et al. Llama 2: Open foundation and fine-tuned chat models. *arXiv preprint arXiv:2307.09288*, 2023. [7](#)
- [46] Can Wang, Menglei Chai, Mingming He, and et al. Clip-nerf: Text-and-image driven manipulation of neural radiance fields. In *CVPR 2022*, pages 3835–3844, 2022. [3](#)
- [47] Chen Wang, Xian Wu, Yuan-Chen Guo, and et al. Nerf-sr: High quality neural radiance fields using supersampling. In *ACM MM 2022*, pages 6445–6454, 2022. [1](#)
- [48] Can Wang, Ruixiang Jiang, Menglei Chai, Mingming He, Dongdong Chen, and Jing Liao. Nerf-art: Text-driven neural radiance fields stylization. *IEEE Transactions on Visualization and Computer Graphics*, 2023. [1](#), [2](#), [3](#), [6](#), [7](#), [14](#)
- [49] Peng Wang, Lingjie Liu, Yuan Liu, Christian Theobalt, Taku Komura, and Wenping Wang. Neus: Learning neural implicit surfaces by volume rendering for multi-view reconstruction. *arXiv preprint arXiv:2106.10689*, 2021. [1](#)
- [50] Fanbo Xiang, Zexiang Xu, Milos Hasan, and et al. Neutex: Neural texture mapping for volumetric neural rendering. In *CVPR 2021*, pages 7119–7128, 2021. [1](#)
- [51] Bangbang Yang, Chong Bao, and Junyi et al. Zeng. Neumesh: Learning disentangled neural mesh-based implicit field for geometry and texture editing. In *ECCV 2022*, pages 597–614. Springer, 2022. [1](#)
- [52] Kai Zhang, Gernot Riegler, Noah Snavely, and Vladlen Koltun. Nerf++: Analyzing and improving neural radiance fields. *arXiv preprint arXiv:2010.07492*, 2020. [1](#)
- [53] Kai Zhang, Nick Kolkin, Sai Bi, Fujun Luan, Zexiang Xu, Eli Shechtman, and Noah Snavely. Arf: Artistic radiance fields. In *European Conference on Computer Vision*, pages 717–733. Springer, 2022. [3](#)
- [54] Jingyu Zhuang, Chen Wang, Lingjie Liu, Liang Lin, and Guanbin Li. Dreameditor: Text-driven 3d scene editing with neural fields. *arXiv preprint arXiv:2306.13455*, 2023. [2](#), [3](#), [7](#), [11](#), [14](#)

LatentEditor: Text Driven Local Editing of 3D Scenes

Supplementary Material

A. Overview

The supplementary material has been organized into the following sections:

- Section **B**: Technical Contribution and Novelty
- Section **C**: Details on S.O.T.A NeRF Editing Methods
- Section **D**: LatentEditor Algorithm
- Section **E**: Adapter Design Details
- Section **F**: Implementation Details
- Section **G**: Additional Results
- Section **H**: User Study

B. Technical Contribution and Novelty

In the proposed LatentEditor framework, our primary focus is on enabling local editing of Neural Radiance Fields (NeRF). To facilitate this, we introduce a novel delta module that assigns delta scores within the latent space. This approach forms the basis of our distinctive technique for training NeRF on real-world 3D scenes within the latent space, capitalizing on the benefits of latent masks for precise editing.

While the concept of training Neural Radiance Fields (NeRF) in the latent space of Latent Diffusion Models was initially introduced by Latent-NeRF [26], their focus was limited to generating 'virtual' 3D objects from textual conditions, rather than real-world 3D data. Our approach, in contrast, represents a novel advancement by training latent space NeRF for authentic 3D scenes. We achieve this by embedding RGB images of real scenes as latent representations and introducing a unique refinement module to enhance reconstruction performance. Training NeRF in the latent space provides benefits like diminished training load and improved editability, leveraging the direct use of output rendered in Latent Diffusion Model (LDM) frameworks.

Our work marks a substantial contribution to the field, demonstrating a significant technical leap in the realm of NeRF research, which has predominantly been focused on training with natural RGB images. This expansion into real 3D scene reconstruction using latent space methodologies is a notable stride in advancing NeRF capabilities.

There exist several NeRF backbone models that facilitate faster training. However, editing a NeRF model in tandem with a Diffusion model necessitates rendering high-resolution imagery (e.g., 512x512) and computing gradients relative to it, which incurs considerable GPU memory use. Our model, trained on lower-dimension data (e.g., 64x64), circumvents this challenge by significantly reducing memory requirements for NeRF fine-tuning. By addressing the core issue of training efficiency through the reduction in

data dimensions, our approach realizes a more resource-efficient training process compared to conventional NeRF models operating in image space.

In summary, LatentEditor exhibits two key attributes for effective NeRF editing: (i) enhanced speed and resource efficiency in the NeRF editing process, and (ii) the ability to perform local editing while maintaining the integrity of the background.

C. Related Work on NeRF Local Editing

Within the domain of neural radiance fields, Instruct-Nerf2Nerf (IN2N) [9] represents a significant step forward by utilizing 2D image translation models, notably Instruct-Pix2Pix (IP2P) [2], for adjusting 2D image features to optimize NeRF training, under the guidance of textual prompts. However, the heavy reliance of IN2N on IP2P for processing NeRF training data occasionally results in over-editing of scenes. To mitigate this, the DreamEditor framework [54] was proposed, introducing a mesh-based neural field method. This strategy enables the conversion of 2D masks to 3D editing zones, allowing for targeted local modifications while preventing unnecessary geometric changes when only altering the visual appearance.

DreamEditor Analysis. DreamEditor [54] employs pre-computed editing masks in tandem with text prompts to streamline the editing workflow. Although DreamEditor claims the use of a diffusion model [38] for mask generation, the specifics of this process remain ambiguous. A thorough examination of their implementation¹ reveals that DreamEditor actually utilizes a pre-trained segmentation model for producing local editing masks, which are included in their provided dataset². Moreover, DreamEditor faces challenges like prolonged training duration and limitations to specific scene types. Moreover, the segmentation models [16, 23] often fail to accurately interpret the editing prompts, necessitating object specification in a singular format for segmentation.

Contrastingly, our method innovates by integrating latent space training in NeRF with a novel delta module that utilizes diffusion models for mask generation. This approach enables accurate local editing without the need for additional guidance. The effectiveness of our method is demonstrated through comparative analyses presented in the main

¹<https://github.com/zjy526223908/dreameditor>

²https://drive.google.com/drive/folders/12_P1C9cd8ZPg3tXrxJ1m-HKAGYDiahjc

paper and the provided videos along with the *supplementary material* highlighting our framework’s enhanced capabilities in local editing compared to other text-driven NeRF methodologies.

D. LatentEditor Algorithm

In this section, we introduce the algorithm underlying our proposed LatenEditor framework.

Algorithm 1 LatenEditor for NeRF Editing

- 1: **Input:** Multi-view image dataset \mathbf{I} , text prompt C_e , editing rate v , training iteration i
 - 2: **Output:** Edited NeRF model F_θ and Adapter F_Θ
 - 3: // Model Initialization
 - 4: Encode \mathbf{I} using encoder \mathcal{E} to obtain $\mathbf{Z} := \{z^n = \mathcal{E}(I^n)\}_{n=1}^N$
 - 5: Train F_θ and F_Θ using loss \mathcal{L}_T with \mathbf{Z}
 - 6: // NeRF Editing
 - 7: **for** $i = 1$ **to** #ofiterations **do**
 - 8: **if** $i/v == 0$ **then**
 - 9: Generate noisy latent $z_{\Delta t}^n$
 - 10: Calculate delta map Δ_ε
 - 11: Generate binary mask M from Δ_ε
 - 12: Generate another noisy version \tilde{z}_t^n
 - 13: Compute edited latent z_e^n
 - 14: Update latent z^n with edited latent z_e^n
 - 15: **end if**
 - 16: **end for**
 - 17: // Optimizing NeRF Editing
 - 18: Update F_θ, F_Θ with modified set \mathbf{Z}_e using loss \mathcal{L}_T
-

E. Adapter Design Details

As previously discussed, the original idea of translating NeRF into latent space was pioneered by Latent-NeRF [26], with an emphasis on creating ‘virtual’ 3D assets. The authors of [26] further enhanced this model by performing fine-tuning in the pixel space, enabling the NeRF model to function directly with RGB values. This was achieved by transforming a NeRF trained in latent space into one operating in RGB space through a linear layer. Such refinement becomes essential due to the unique architecture of the encoder and decoder in Stable Diffusion [38], which utilize ResNet blocks and self-attention layers, leading to intricate interactions among pixel values during the conversion from image to latent space.

As we aim to train NeRF in latent space, converting images to latents creates a misalignment between latent and image pixel values, as NeRF’s rendering method independently computes pixel values through an MLP, devoid of inter-pixel interaction.

In response to this challenge and to better adapt our latent editing approach to 3D real-world scenes, we have developed a specific refinement module. This module is distinguished by a trainable adapter that eliminates the necessity of transitioning from latent space to RGB for refinement. While adapters have been widely studied in the context of vision transformers [4, 14, 44], our adapter is uniquely tailored to incorporate the inter-pixel interactions inherent to ResNet and self-attention mechanisms. This integration substantially improves the reconstruction quality. The designed adapter has nearly 0.28 million parameters.

E.1. Adapter Design Variants

The benefits of the refinement module are elaborated upon in the main text of the paper. As distinctly illustrated in the ablation section of the main paper, there is a noticeable enhancement in rendering quality attributable to this module. The development of the refinement module was preceded by an empirical analysis of multiple architectural designs, the comparative results of which are presented in Table 1.

Adapter Type	CLIP Text-Image Direction Similarity \uparrow	CLIP Direction Consistency \uparrow	Edit PSNR \uparrow
w/o Residual	0.2685	0.9572	23.15
w/o Self-attention	0.2503	0.9351	22.89
Ours	0.2801	0.9881	26.47

Table 1. Quantitative evaluation of various adapter variants. We analyze the adapter without a residual connection and self-attention. Both design variants fail to match the performance of the proposed design. We use the same set of 14 scenes and 56 edits as we discussed in the main paper for this experiment.

F. Implementation Details

We set $\lambda_r = 0.85$ and $\lambda_f = 0.15$ for the initial 2500 steps in model initialization and 400 steps in NeRF editing stages. For the remaining steps, we set $\lambda_r = 1.0$ and $\lambda_f = 0.0$. For NeRF editing, we use $s_T = 7.5$ and $s_I = 1.5$ in all of our experiments. For the threshold, we set $\mu = 0.45$. For all other experimental settings and model configurations, we use the default settings of [9].

F.1. Model Initialization - Efficiency Analysis

The primary advantage of training the Nerfacto model [43] in latent space, rather than pixel space, lies in the significantly lower resolution of latent representations compared to RGB images. Specifically, the Stable Diffusion [38] VAE used in our study downscales an input image of resolution $W \times H \times 3$ to latents of size $H/8 \times W/8 \times 4$. As a result, the latent Nerfacto model processes 64 times fewer rays than its RGB counterpart. Theoretically, this reduction allows for training with a batch size (# of rays) 64 times smaller while keeping the number of model initialization training iterations constant (30,000 iterations, as in IN2N [9]), leading to a substantially smaller memory footprint. Alterna-

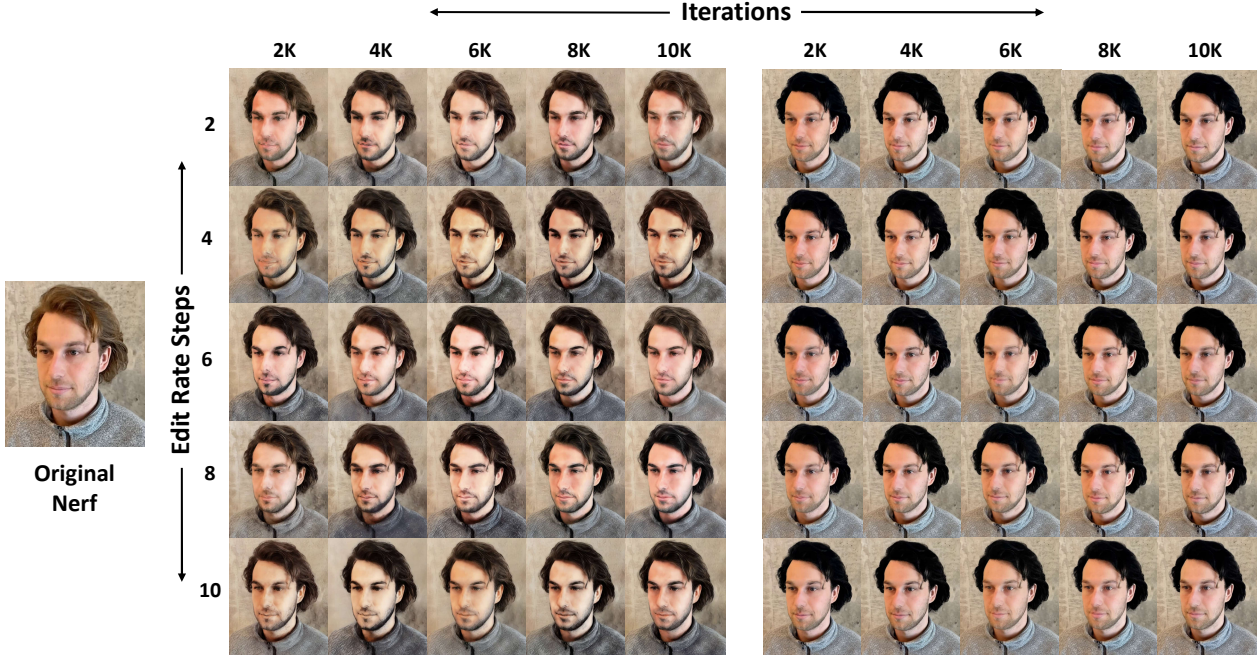


Figure 1. This figure provides a comparative analysis between *LatentEditor* and IN2N [9], focusing on computational efficiency across different editing rates. The aim is to reduce the number of required training iterations for higher editing rates (less frequent IP2P calls). Extending the comparison presented in ablations of the main paper, where we used a default editing rate of 10, this figure explores editing rates ranging from 2 to 10 and documents the outcomes for various numbers of fine-tuning iterations. *LatentEditor* demonstrates effective editing within approximately 2000 iterations, while IN2N struggles to achieve comparable results even after 10,000 iterations.

tively, one could maintain the same batch size as the RGB model (in IN2N [9]) and reduce the number of iterations by a factor of 64 to achieve effective latent output. However, in our experiments, we chose a batch size of 1,024 and trained for 30,000 iterations. Under this setup, our models require 1,236MB of GPU memory (including memory for the Refinement Adapter), in contrast to the 2,086MB needed by the RGB model as indicated in Table 2. In terms of time efficiency, our complete training pipeline, which includes latent generation, training the latent Nerfacto, and training the Refinement Adapter (1,000 iterations), is completed in 758 seconds. These results were obtained using the “fangzhou-small” scene from IN2N [9] dataset on NVIDIA RTX 4090 GPU. However, in our analysis, we observe that *LatentEditor* can achieve similar results with the initial training of 15,000 iterations bringing the total training time below 400 seconds, significantly faster than the 745 seconds required by the Nerfacto model in IN2N [9].

Method	Nerfacto Training	Adapter Training	Total Memory
IN2N [9]	2086 MB	-	2086 MB
<i>LatentEditor</i>	1158 MB	78 MB	1236 MB

Table 2. Comparison of GPU Memory Consumption between IN2N and the proposed *LatentEditor* Using the Nerfacto Model during model initialization stage

F.2. NeRF Editing - Efficiency Analysis

When considering the “fangzhou-small” scene from the IN2N dataset [9], the batch size set during editing is 16,384, corresponding to the original RGB image dimensions of 512×320 in the IN2N implementation. In this configuration, the NeRF model alone demands approximately 6,778 MB of GPU memory, excluding the additional memory required by the diffusion model. On the other hand, *LatentEditor*, leveraging latent dimensions of 64×40 for the “fangzhou-small” image latents, permits a reduced batch size of 2,560. This adjustment significantly reduces the NeRF model’s memory usage to 1,766 MB.

In addition, *LatentEditor* requires less number of fine-tuning iterations. Figure 1 presents a comparative analysis of *LatentEditor* and IN2N [9] on the “face” scene of the IN2N dataset [9], examining computational efficiency across various editing rates. This figure extends the analysis from the ablation study in the main paper, which used a default editing rate of 10, by exploring rates from 2 to 10 and recording the number of fine-tuning iterations. *LatentEditor* efficiently achieves editing goals within about 2000 iterations, in contrast to IN2N, which requires over 10,000 iterations for similar results. This ablation study highlights the superior efficiency of *LatentEditor* in terms of required training iterations, achieving a 5 to 10-fold reduction com-



Figure 2. This figure presents a comparison of LatentEditor, IN2N, and Control4D in terms of local and multi-attribute editing. The comparison reveals that Control4D modifies the original scene content. IN2N, while editing, inadvertently alters unintended regions, such as changing the beard and jacket color when only a hair color change is intended. In contrast, LatentEditor successfully accomplishes the desired editing outcomes as specified by the given prompts.

pared to IN2N, despite the increased cost per step due to multiple denoising stages. Consequently, *LatentEditor* is **5-8** times faster in NeRF editing than IN2N.

F.3. Efficient Rendering

Using the LLFF dataset as a benchmark, Nerfacto requires an average of 2.85 seconds to render a single image at 512 resolution. In comparison, our model, which first renders a latent feature map and then decodes it to an RGB image, takes only an average of 1.35 seconds per image. This efficiency gain, amounting to a 2.1-fold reduction in inference time, is attributed to the training in latent space and the lowered resolution employed by LatentEditor.

G. Additional Results

We present the outcomes of style transfer, local editing, and multi-attribute editing applications. Our methodology is compatible with any generative models specialized in object removal or inpainting, facilitating the required local editing. While this paper primarily focuses on demonstrating our method’s core capabilities, it does not include results for object removal or inpainting in 3D scenes. This omission aligns with the baseline method presented in [9], which also does not address these specific tasks.

G.1. Qualitative Results

We further present the qualitative comparisons with Control4D [41] and DreamEditor [54] in Figure 2. Figure 2 illustrates the contrasts in local and multi-attribute editing among LatentEditor, IN2N, and Control4D. As the Control4D [41] code is not publicly accessible, we developed an in-house implementation to assess the impact of GAN guidance. Control4D tends to alter the original scene content, while IN2N inadvertently changes unintended areas, like beard and jacket color when only a hair color change is intended. Conversely, LatentEditor precisely achieves the editing objectives as per the prompts, demonstrating its superior accuracy in targeted modifications.

Moreover, Figure 3 compares LatentEditor with NeRF-Art [48], DreamEditor [54], and IN2N [9], focusing on style transfer capabilities. LatentEditor distinguishes itself by achieving the desired style transfer results in significantly fewer training iterations, about 3000, compared to IN2N, which requires approximately 18000 iterations. This efficiency in obtaining high-quality outcomes with fewer iterations highlights the practical utility of LatentEditor in style transfer applications.

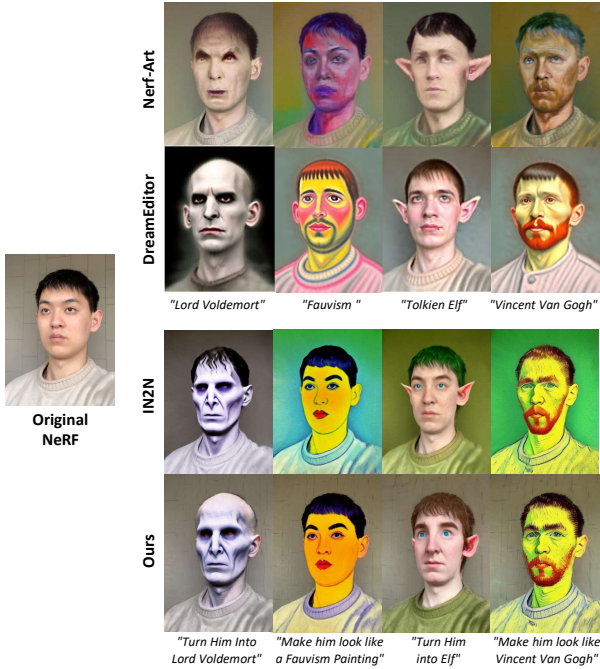


Figure 3. This figure compares LatentEditor with Nerfart, DreamEditor, and IN2N. LatentEditor stands out by achieving the targeted style transfer outcomes with a significantly lower number of training iterations (approximately 3000), showcasing a notable efficiency advantage over IN2N (requires about 18000 iterations).

G.2. Quantitative Evaluation Metrics

In our quantitative evaluation, we utilize three metrics: the *CLIP Text-Image Direction Similarity* [6], the *CLIP Direction Consistency Score* [9], and *Edit PSNR*. The CLIP Directional Score evaluates the alignment between the textual caption changes and the corresponding image transformations. In contrast, the CLIP Consistency Score assesses the cosine similarity between the CLIP embeddings of consecutive frames along a novel camera trajectory. The Edit PSNR metric evaluates the cosine similarity and PSNR (Peak Signal-to-Noise Ratio) for each rendered view, comparing the edited NeRF against the input NeRF. This comparison demonstrates that our method maintains greater consistency in the edited scene with respect to the original input scene.

Method	CLIP Text-Image Direction Similarity \uparrow	CLIP Direction Consistency \uparrow	Edit PSNR \uparrow
IP2P [2]+SAM [16]	0.2685	0.9572	20.15
IN2N [9]+SAM [16]	0.2865	0.9851	25.89
LatentEditor	0.2801	0.9881	26.47

Table 3. Quantitative evaluation by using pre-trained segmentation model with IN2N and IP2P. We use the same set of 14 scenes and 56 edits as we discussed in the main paper for this experiment.

G.3. Comparing with Mask+IP2P

We further evaluate LatentEditor by combining a pre-trained segmentation model SAM [16] with IN2N [9] and IP2P [2]. The quantitative results are presented in Table 3.

H. User Study Details

To assess the perceptual preferences of human subjects towards edited NeRF renderings, we conducted a comprehensive user study. This study involved rendering images from 8 distinct scenes taken from the LLFF, IN2N, and NeRFstudio datasets. Feedback was solicited from 500 participants, whose ages ranged from 18 to 68 years. During the study, each participant was shown a series of multi-view renderings generated by our model and various baseline models. The presentation order of these renderings was randomized to ensure unbiased feedback.

Participants were asked to rate each rendering using a preference scoring survey, with the scoring scale ranging from 1 (very low) to 10 (very high), encompassing five distinct rating options. The study aimed to evaluate three key aspects of the edited NeRF renderings:

1. **Text Fidelity:** Whether the image accurately reflects the target text condition.
2. **Content Preservation:** The model’s effectiveness in precisely editing the targeted object.
3. **Scene Consistency:** The degree to which the 3D scenes maintain consistency across different views.

The aggregated results of this user study are presented in the main paper. Our method demonstrated superior performance in terms of text fidelity and content preservation, achieving the highest scores in these categories. Additionally, it ranked second in scene consistency, underlining its effectiveness in maintaining view coherence. Overall, our approach surpassed the baseline models in terms of perceptual quality, as reflected in the user feedback.